MedChemComm

Accepted Manuscript

This article can be cited before page numbers have been issued, to do this please use: H. Tye, S. Zahn, M. Hofmann, M. Sanderson, O. Schaff, M. Troy, M. Mayer, G. Rast, S. Pal and U. Guertler, *Med. Chem. Commun.*, 2015, DOI: 10.1039/C5MD00097A.

This is an *Accepted Manuscript*, which has been through the Royal Society of Chemistry peer review process and has been accepted for publication.

Accepted Manuscripts are published online shortly after acceptance, before technical editing, formatting and proof reading. Using this free service, authors can make their results available to the community, in citable form, before we publish the edited article. We will replace this *Accepted Manuscript* with the edited and formatted *Advance Article* as soon as it is available.

You can find more information about *Accepted Manuscripts* in the Information for Authors.

Please note that technical editing may introduce minor changes to the text and/or graphics, which may alter content. The journal's standard Terms & Conditions and the Ethical guidelines still apply. In no event shall the Royal Society of Chemistry be held responsible for any errors or omissions in this *Accepted Manuscript* or any consequences arising from the use of any information it contains.

ROYAL SOCIETY OF CHEMISTRY

www.rsc.org/medchemcomm

Title

Discovery of novel amino-pyrimidine inhibitors of the insulin-like growth factor 1 (IGF1R) and insulin receptor (INSR) kinases; parallel optimization of cell potency and hERG inhibition

Authors

Heather Tye[a]*, Ulrich Guertler[c], Marco H. Hofmann[b], Moriz Mayer[b], Sandeep Pal[a], Georg Rast[c], Michael P. Sanderson[b], Otmar Schaaf[b], Matthias Treu[b], Stephan K. Zahn[b]

(a) Evotec (UK) Ltd, 114 Innovation Drive, Milton Park, Abingdon, Oxfordshire OX14 4SA, UK
(b) Boehringer Ingelheim RCV GmbH & Co KG, Dr.-Boehringer-Gasse 5-11, 1120 Vienna, Austria
(c) Boehringer Ingelheim Pharma GmbH & Co. KG, Birkendorfer Str. 65, 88397 Biberach / Riß, Germany

Abstract

The insulin-like growth factor-1 receptor (IGF1R) and closely related insulin receptor (INSR) are receptor tyrosine kinases which have been postulated to play a role in the tumorigenesis of certain cancers. Strategies for inhibiting oncogenic signaling via the IGF1R and INSR include IGF1R antibodies, IGF1/2 antibodies and dual IGF1R/INSR tyrosine kinase inhibitors (TKIs). IGF1R/INSR TKIs linsitinib (OSI-906) and BMS-754807 have progressed to phase II/III clinical studies in cancer patients. We describe here our efforts to develop small molecule dual inhibitors of the IGF1R/INSR receptor kinases based on an amino-pyrimidine structural class. Our main focus was the parallel optimization of cellular potency and off target activity (principally hERG inhibition) through modulation of physicochemical properties and introduction of key structural motifs using a matched molecular pairs approach and hERG homology model.

Introduction

The insulin-like growth factor-1 receptor (IGF1R) and closely related homolog the insulin receptor (INSR) are receptor tyrosine kinases which have been postulated to play a role in the tumorigenesis of certain cancers.[1] Engagement of the receptors by their cognate ligands (IGF1, IGF2 and insulin) leads to auto-phosphorylation of specific intracellular domain tyrosine residues. The docking of effector proteins, such as IRS-1, to these phospho-tyrosines activates signal transduction via the Ras/Raf/MAPK and PI3K/AKT/mTOR pathways and promotion of oncogenic cellular responses including proliferation, cell growth and survival.[2] As such, much interest has been devoted towards the development of therapeutic agents targeting the function of the IGF1R and INSR.

Strategies for inhibiting oncogenic signaling via the IGF1R and INSR include IGF1R antibodies[3],IGF1/2 antibodies[4] and dual IGF1R/INSR tyrosine kinase inhibitors (TKIs).[5] The efficacy of IGF1R antibodies in clinical studies, which target the IGF1R meanwhile sparing the INSR, has been mostly disappointing.[6] Preclinical data suggests that co-targeting of the IGF1R and INSR, using small molecule kinase inhibitors, more broadly inhibits the pathway and is associated with greater anti-tumor efficacy.[7] Amongst the IGF1R/INSR TKI inhibitor class, linsitinib (OSI-906) and BMS-754807 (Figure 1a) have progressed to phase II/III clinical studies in cancer patients. Preclinical data have indicated that BMS-

View Article Online
DOI: 10.1039/C5MD00097A

754807 is a potent inhibitor of the IGF1R and INSR with IC50 values of 1.8 and 1.7 nM, respectively. Additional kinases are also inhibited with IC50 values below 50 nM including TrkA, TrkB, c-Met, RON, Aurora A and Aurora B. Thus BMS-754807 is somewhat less specific than linsitinib (OSI-906), which displays potent and selective inhibition of only IGF1R and INSR.[5,8]

Figure 1a – Literature IGF1R Inhibitors

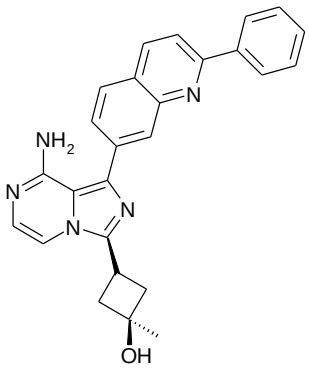

Linsitinib

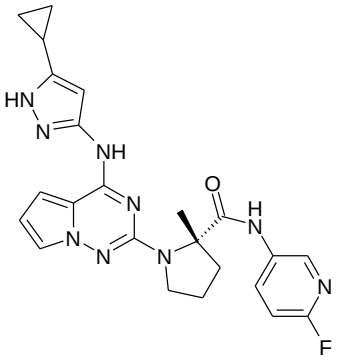

BMS-754807

We describe here our efforts to develop small molecule dual inhibitors of the IGF1R/INSR receptor kinases based on an amino-pyrimidine structural class. Our main focus was the modulation of physicochemical properties and introduction of structural motifs which would enable optimization of cellular potency and off target activity (principally hERG inhibition) in parallel.

Results and discussion

During follow-up activities from an HTS campaign to identify small molecule dual inhibitors of the IGF1R/INSR kinases, we identified a novel class of amino-pyrimidine analogues bearing an amino benzyl oxindole substituent on the pyrimidine ring (Figure 1b). Compounds of this type were found to be dual IGF1R/INSR inhibitors (assessment of a number of early compounds showed no selectivity between IGF1R and INSR activity, data not shown) with modest activity in cell lines dependent on IGF1R/INSR signaling (e.g. TC-177 and TC-71) and little activity in cells lacking IGF1R/INSR dependence (e.g. HCT 116) (Table 1). The binding mode of this class of compound (as determined for a closely related structural class, unpublished results) was as expected with the amino-pyrimidine motif making key hydrogen bonding interactions with the hinge region of the ATP binding pocket.

Figure 1b – Pyrimidine analogues 1-8

View Article Online
DOI: 10.1039/C5MD00097A

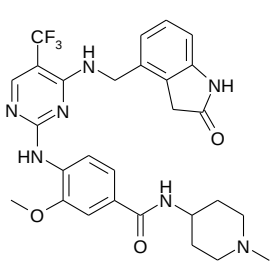

1

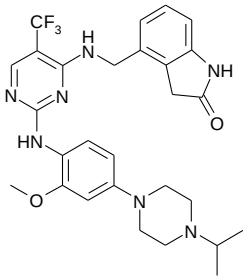

2

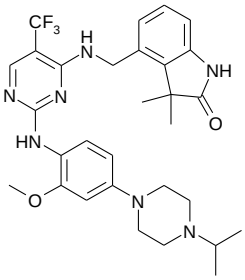

3

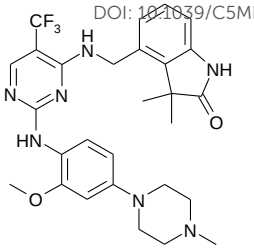

4

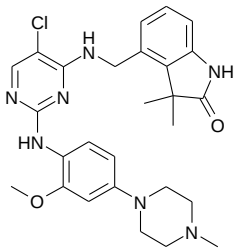

5

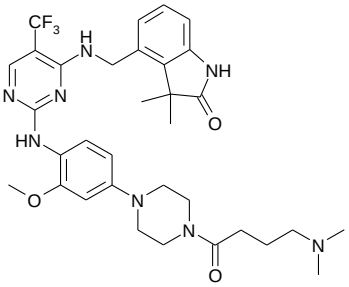

6

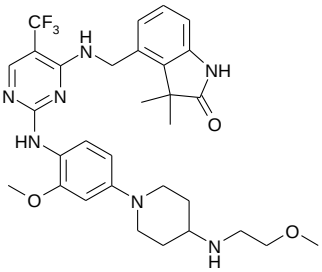

7

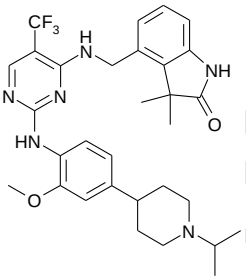

8

Table 1 – Kinase and cell potencies for analogues 1-4

Compound Number	IGF1R[a] IC_{50} [nM]	TC177[b] EC_{50} [nM]	HCT116[c] EC_{50} [nM]
(1)	14	216	3475
(2)	9	97	895
(3)	1	61	3222
(4)	1	66	1968

Table 1 footnote:

(a) Mean IC_{50} values. Variation typically +/- 50% based on control compound IC_{50} 69 nM, SD 34, n of 80. Control compound was a non-specific ATP competitive kinase inhibitor tool compound from Boehringer Ingelheim

(b) Mean ECC_{50} values. Variation typically +/- 50% based on control compound EC_{50} 31 nM, SD 18, n of 5. The control compound used for all cell proliferation assays was a broadly cytotoxic tool compound from Boehringer Ingelheim

(c) Mean EC_{50} values. Variation typically +/- 50% based on control compound EC_{50} 5 nM, SD 3, n of 307. The control compound used for all cell proliferation assays was a broadly cytotoxic tool compound from Boehringer Ingelheim

An early optimization objective was to improve the cellular potency of this class of compounds. Replacement of the polar amide motif in compound 1 with a piperazine resulted in an improvement in cell potency (compound 2) but this was accompanied by a loss in cellular window with respect to HCT 116 activity. A relatively high dose of 100 mg/kg p.o. (qd) was necessary to achieve a modest tumor growth inhibition (TGI) of 59% in a subcutaneous allograft model (3T3-hIGF1R). The cellular window could be regained by modification of the oxindole motif giving rise to a series of compounds with a good cell window and acceptable cell potency (e.g. compounds 3 and 4). PK profiling revealed

compound 4 as a suitable tool compound with good oral exposure which could be used for profiling in an efficacy model (see Table 4). A dose of 75 mg/kg p.o. (qd) of compound 4 delivered TGI values of 71% and 103% in the 3T3-hIGF1R allograft and subcutaneous GEO xenograft models, respectively (Table 5).

Encouraged by this result we sought to further optimize this compound with the goal of increasing efficacy at a reduced dose by further improving the cellular potency. However, following additional profiling of compound 4 we discovered that it was a potent inhibitor of the hERG potassium channel (IC_{50} = 160 nM). From a CV safety perspective we considered a window between the hERG IC_{50} and the unbound Cmax of >30 fold to be a minimum requirement. For compound 4 with an unbound Cmax of 16 nM (based on Cmax 2600 nM, PPB 99.4%, see table 4) this window was only 10 fold. With the expectation that the PK profiles of compounds in the series would be broadly similar we set an objective of increasing the hERG IC_{50} to at least 1 μM to be sure of achieving the desired window. This led to the dual objective of optimizing cellular potency and hERG inhibition in parallel.

Compound 4 and the related 5-trifluoromethyl-2,4-diaminopyrimidines can be synthetically accessed via the procedure shown in Figure 2 starting from 5-trifluoromethyl-2,4-dichloro-pyrimidine and subsequent nucleophilic aromatic substitution as described by co-workers at Pfizer.[9] For the 5-trifluoromethyl series the regioselective introduction of the R2-aniline is catalyzed and facilitated by zinc (II)-chloride. In the 5-halogen series the R4-amine can be introduced first with high regioselectivity under basic conditions. Further details of synthetic routes are included in the supporting information.

Table 2 – Kinase, cell, hERG and physicochemical properties for analogues 4-8

Compound Number	IGF1R[a] IC_{50} [nM]	TC177[b] EC_{50} [nM]	HCT116[c] EC_{50} [nM]	hERG IC_{50} ±SD [nM]	logD[d] pH 7.4	Calc. pKa[e]
(4)	1	66	1968	166±13	4.3	7.8
(5)	2.5	122	2843	996±65	4.0	7.8
(6)	1.5	140	3160	> 3000	2.2	n.a.
(7)	0.2	36	1637	3186±171	2.3	9.7
(8)	0.4	59	1663	n.d.	3.9	9.6

Table 2 footnote:

(a) Mean IC_{50} values. Variation typically +/- 50% based on control compound IC_{50} 69 nM, SD 34, n of 80. Control compound was a non-specific ATP competitive kinase inhibitor tool compound from Boehringer Ingelheim
(b) Mean ECC_{50} values. Variation typically +/- 50% based on control compound EC_{50} 31 nM, SD 18, n of 5. The control compound used for all cell proliferation assays was a broadly cytotoxic tool compound from Boehringer Ingelheim
(c) Mean EC_{50} values. Variation typically +/- 50% based on control compound EC_{50} 5 nM, SD 3, n of 307. The control compound used for all cell proliferation assays was a broadly cytotoxic tool compound from Boehringer Ingelheim
(d) logD values calculated using Chemaxon software
(e) pKa values calculated using Chemaxon software

View Article Online
DOI: 10.1039/C5MD00097A

Figure 2 – Synthetic routes

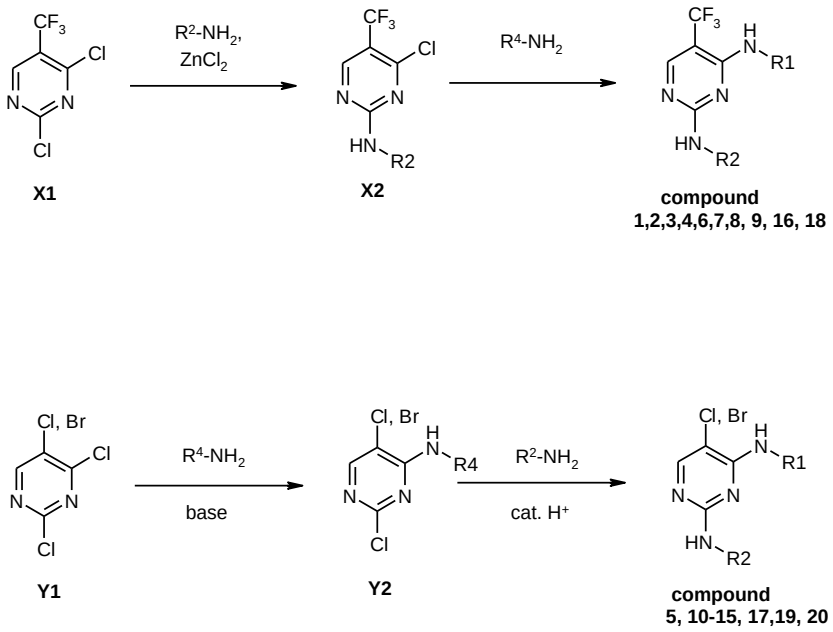

Figure 2 footnote:

For conversion X1 to X2: typical scale 1 – 15 g, yields approx. 50 – 90%; X2 to compound: typical scale0.05 to 5 g, yields approx. 50 to 80%.

For conversion Y1 to Y2: typical scale 0.5 to 5 g, yields approx. 60 - 85%; Y2 to compound or intermediate for final decoration: typical scale 0.05 to 1 g, yields 50 – 90%

Common strategies for reducing the hERG inhibition potential of compounds include reducing lipophilicity, reducing basicity and/or altering the position of the basic center relative to the lipophilic motif(s).[10] We decided to explore all of these options in parallel by preparing a limited number of compounds in which either lipophilicity (replacing CF_3 with Cl in compound 5) or the nature of the basic solubilizing group was altered (compounds 6 and 7). Both approaches resulted in a reduction in hERG inhibition (see Table 2) however the incorporation of an amide motif (compound 6) led to an undesirable reduction in cell potency. Switching from a piperazine to an amino piperidine (compound 7) proved to be favorable in terms of both cell potency and hERG inhibition.

At this point in our optimization campaign it was decided that it would be preferable to change the linkage (X in figure 4) of the solubilizing motif from a nitrogen atom to a carbon atom. This was done to mitigate the risk of releasing a potentially mutagenic aniline upon metabolism of the piperazine or amino piperidine ring. Compound 8 was prepared to verify that such a change would be tolerated with respect to IGF1R inhibition. This was indeed found to be the case with compound 8 retaining a good level of cell potency and cellular window (see table 2).

To assist in the design of further analogues we decided to employ a homology model of the hERG ion channel. To this end we reproduced a model of the open form of the hERG channel described by Aqvist[11] into which we docked compound 4 (see Figure 3). The resultant docked pose suggested that a key interaction was made between the basic center of compound 4 and serine residues in the selectivity pocket. This was in agreement with our experimental observation that altering the basicity or position of this motif had an impact on the level of hERG inhibition. The side chain from the basic motif protruded into a strongly electronegative region of the hERG channel suggesting that introduction of electronegative groups at this position may further disrupt binding to the hERG channel.

Figure 3 – Schematic of hERG model for compound 4

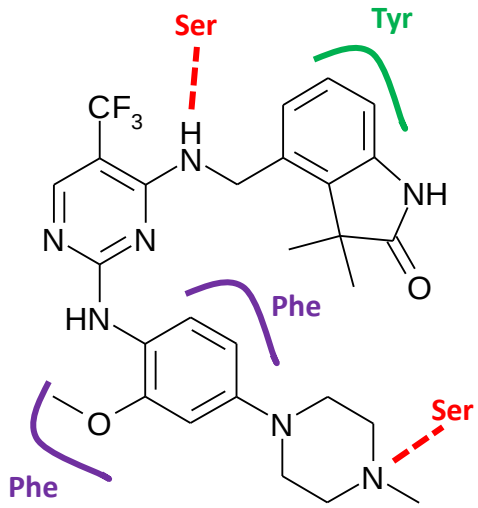

Figure 4 – Scaffold and R groups for analogues 9-20

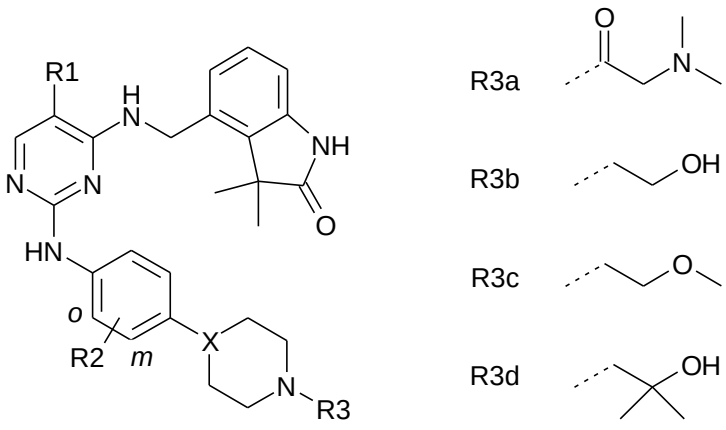

Based on the results of the hERG modelling and the data obtained so far the best approach was considered to be variation of R1, R2 and R3 in parallel to provide molecules with reduced logD and

View Article Online
DOI: 10.1039/C5MD00097A

bearing motifs at R3 which could reduce the hERG inhibition potential either by modulating basicity or introducing electronegative side chains (Figure 4). A number of analogues were prepared following a matched molecular pairs approach[12] to aid in data interpretation; Plot 1 shows the relationship between pIC_{50} and logD for either IGF1R or hERG inhibition of these compounds. Whilst there was a clear trend towards reduced hERG activity at reduced logD there was no apparent relationship between IGF1R activity and logD. This gave us confidence that it should be possible to identify potent IGF1R inhibitors with reduced hERG liability within this chemical series. The remaining challenge was then to achieve this whilst maintaining cellular potency.

Plot 1 – Relating hERG and IGF1R potency to logD

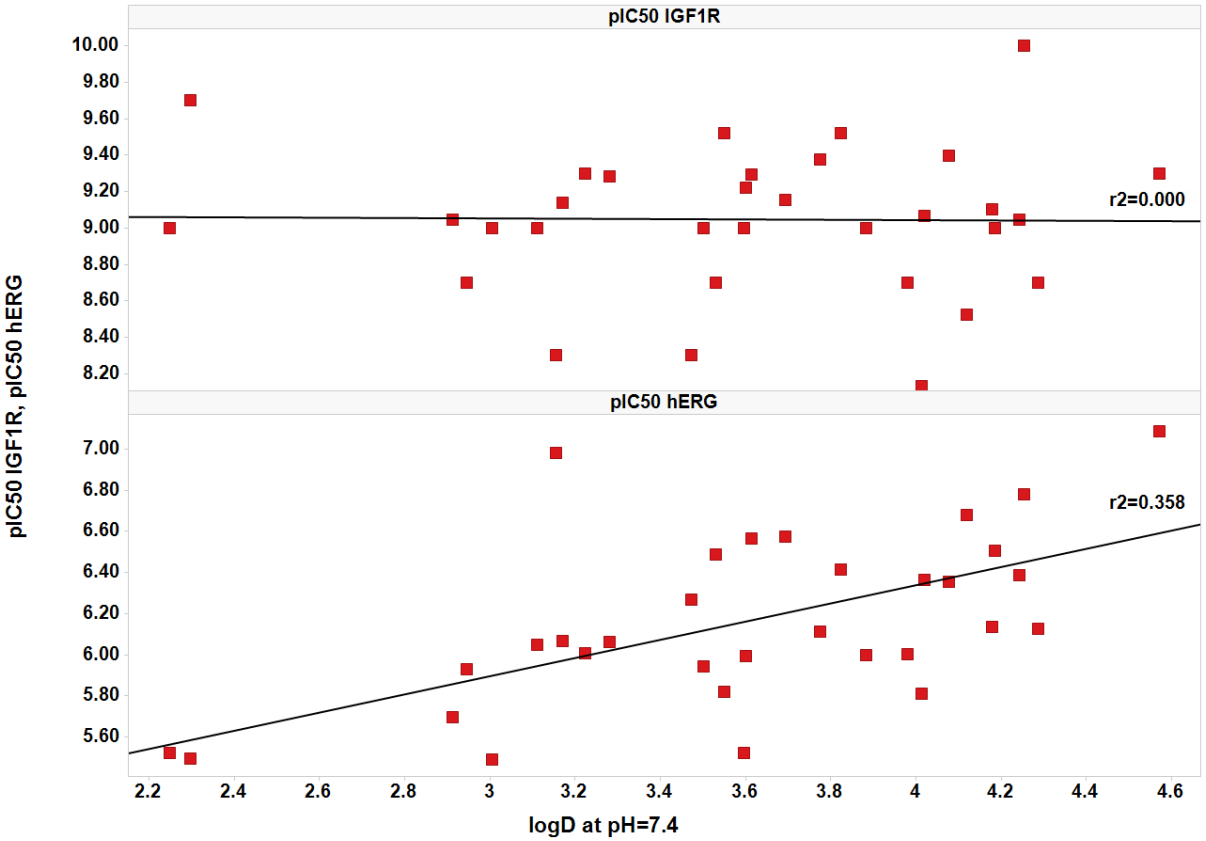

Plot 1 Footnote:

Plot relating pIC50 IGF1R to logD shows no correlation ($R^2 = 0$); Plot relating pIC50 hERG and logD shows some correlation ($R^2 = 0.36$), indicating that optimization of hERG inhibition can be achieved by modulation of logD.

Table 3 summarizes the data for a subset of analogues for which cell data was obtained. For each R3 modification the matched molecular pairs (varying R1) were prepared. In all cases the less lipophilic R1 = Cl analogue proved to have the better hERG profile, this came at the expense of a slight reduction in potency in the IGF1R kinase assay, although the effect on cell potency was relatively neutral (see data for pairs 9 &11, 16&17, 18&20). In fact only the Cl analogues were found to inhibit hERG in the desirable range of $IC_{50} > 1\ \mu M$.

Table 3 – Kinase, cell, hERG and physicochemical properties for analogues 4 and 9-20

Compound Number	X	R1	R2	R3	IGF1R[a] IC_{50} [nM]	TC177[b] EC_{50} [nM]	HCT116[c] EC_{50} [nM]	hERG IC_{50} ±SD [nM]	logD pH 7.4[d]	Calc. pKa[e]
(4)	N	CF_3	*o*-OMe	Me	1	66 (22*)	1968	166±13	4.3	7.8
(9)	C	CF_3	H	a	1.5	330	1755	749±12	4.3	n.a.
(10)	C	Br	H	a	0.8	80	2772	736±49	4.2	n.a.
(11)	C	Cl	H	a	7.4	260	>2500	1541±70	4.0	n.a.
(12)	C	Br	H	b	1.0	118 (54*)	1820	898±46	3.1	9.0
(13)	C	Cl	H	b	2.1	135	1413	1165±54	2.9	9.0
(14)	C	Br	H	c	0.7	94 (57*)	1080	267±14	3.7	9.1
(15)	C	Cl	H	c	2.4	107 (51*)	1127	325±27	3.5	9.1
(16)	C	CF_3	*o*-Me	d	0.3	9*	1704	387±15	3.8	9.5
(17)	C	Cl	*m*-Me	d	0.6	9*	649	1179±60	3.5	9.5
(18)	C	CF_3	*o*-OMe	d	0.5	8*	1745	867±46	3.3	9.5
(19)	C	Br	*o*-OMe	d	0.9	9*	1353	858±33	3.2	9.5
(20)	C	Cl	*o*-OMe	d	1.1	15*	2302	3229±113	3.0	9.5

Table 3 footnote:

(a) Mean IC_{50} values. Variation typically +/- 50% based on control compound IC_{50} 69 nM, SD 34, n of 80. Control compound was a non-specific ATP competitive kinase inhibitor tool compound from Boehringer Ingelheim

(b) Mean ECC_{50} values. Variation typically +/- 50% based on control compound EC_{50} 31 nM, SD 18, n of 5. The control compound used for all cell proliferation assays was a broadly cytotoxic tool compound from Boehringer Ingelheim

(c) Mean EC_{50} values. Variation typically +/- 50% based on control compound EC_{50} 5 nM, SD 3, n of 307. The control compound used for all cell proliferation assays was a broadly cytotoxic tool compound from Boehringer Ingelheim

(d) logD values calculated using Chemaxon software

(e) pKa values calculated using Chemaxon software

Based on earlier data for compound 6 the introduction of an amide group at R3 (R3a) was expected to lead to reduced hERG inhibition. This was indeed the case, with compounds 9-11 showing the better profile; however, as with compound 6, this came at the expense of reduced cellular potency. An alternative approach was to incorporate a polar group at R3 (e.g. R3b) resulting in a reduction in logD. Compounds 12 and 13 showed a reduction in hERG inhibition and retained IGF1R activity but again the cellular potency was reduced. Initially, we believed this to be as a result of the H-bond donor motif, however, the methyl ether R3c (compounds 14 and 15) showed similar activity in the

View Article Online
DOI: 10.1039/C5MD00097A

cellular assay and in fact had dramatically increased hERG inhibition. Based on our earlier modelling we concluded that the OH group in R3b may be giving rise to an electrostatic repulsion in the hERG selectivity pocket. We decided to retain this feature in R3 and use substitution alpha to the OH (R3d) along with variations at R1 and R2 to tune the lipophilicity in the hope of achieving improved cellular potency.

Compound 16 gave the first indication that such an approach could provide compounds with cell potency in the 10 nM range. Incorporation of the R1 = Cl group (compound 17) lead to a reduction in logD which resulted in good cellular potency combined with acceptable hERG inhibition. Modification of the R2 group to methoxy provided compounds with a further reduced logD which retained cellular potency and had a good cellular window (with respect to HCT 116) and reduced hERG inhibition. Compounds 17 and 20 had the best overall profile close to our objective of single digit nanomolar cellular potency combined with hERG inhibition at IC_{50} > 1 µM.

PK profiling of compounds 17 and 20 revealed that they had good oral exposure in mice with a similar profile to compound 4 (Table 4). Both compounds were considered to have suitable CV safety profiles with hERG to unbound Cmax ratios >100 fold. In the 3T3 allograft compound 20 resulted in a TGI of only 52% following 22 days at the 75 mg/kg daily dose; for this reason only compound 17 was subjected to further profiling.

Table 4 - PK data for analogues 4, 17 and 20

Compound Number	PK Mouse *p.o.*				PPB Mouse
	Dose (mg/kg)	Cmax (nM)	tmax (h)	AUC (nM·h)	(% bound)
(4)	50	2600	1.5	34000	99.4
(17)	40	2000	1.2	24000	≥ 99.9
(20)	50	4500	0.5	45000	≥ 99.9

Table 5 – Subcutaneous Allo- and Xenograft studies

Compound Number	Dose (mg/kg) qd, p.o.	TGI in 3T3 (%)	TGI in GEO (%)	TGI in RD-ES (%)
(2)	100	59	-	-
(4)	75	71	103	-
(4)	25	-	63	-
(17)	75	69	-	-
(17)	50	-	98	82
(20)	75	52	-	-

Table 5 Footnote:

Treatment of mice bearing subcutaneous 3T3, GEO or RD-ES tumors. The highest tested dose is defined as maximum tolerated dose (MTD) of a compound and was defined in a two weeks tolerability study prior to the efficacy experiment. Compound 4, which was considered as suitable tool compound and compound 17 were tested in more than one Allo- or xenograft model.

Compound 17 was tested in a kinase panel to determine its selectivity profile (see table 6). Only 6 of the kinases in panel showed >50% inhibition at 1μM and for all of these a >100 fold selectivity window for IGF1R relative to the kinase in question was obtained.

Table 6 – Kinase panel data for compound 17

Kinase	IC_{50} [nM]
ABL1	227
ACVR1B	-
AKT2	-
AMPKA1B1G1	462
CDK2	-
CHEK1	-
CSNK1A1	-
CSNK1A2	-
EGFR	-
EPHB2	-
FGFR1	244
FRAP1 (MTOR)	-
GSK3B	-
LCK	142
MAP2K1	-
MAP3K8	-
MAPK14	-
MAPKAPK2	-
MYLK2	-
NEK2	-
PAK4	-
PDK1	-
PRKACA	-
RAF1	-
ROCK2	-
CAMK2D	150
SRPK2	-
SRK3	-
STK6	117
TBK1	-

Table 6 Footnote:

Compounds tested in panel of kinases; IC_{50}s obtained where compound 17 showed greater than 50% inhibition at 1μM

Daily dosing of compound 17 with 50 mg/kg dose in the GEO model resulted almost in tumor stasis with a TGI of 98% on day 24 (Table 5, Plot 2i). Compared to the control group the mice showed mild diabetes related phenotypes (polyurea and polydipsia) with this dose starting from day 8 but this was not connected with body weight loss (Plot 2ii). Efficacy was also observed in the IGF1R dependent Ewing's Sarcoma model (RD-ES, 82% TGI at the 50 mg/kg dose, table 5) and in the 3T3 allograft (69% TGI at the 75 mg/kg dose, table 5).

Plot 2 – GEO xenograft data for compounds 4 and 17

View Article Online
DOI: 10.1039/C5MD00097A

i)

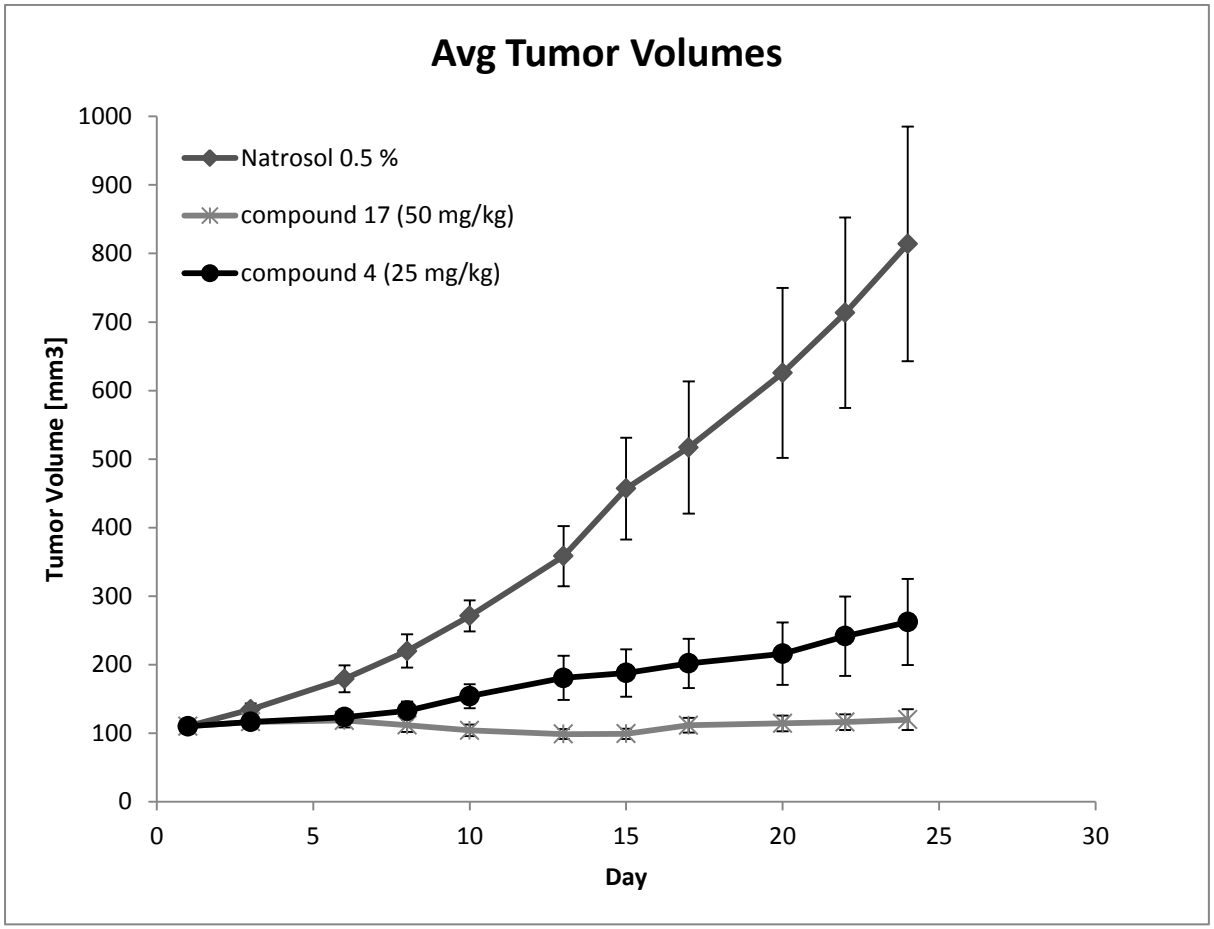

ii)

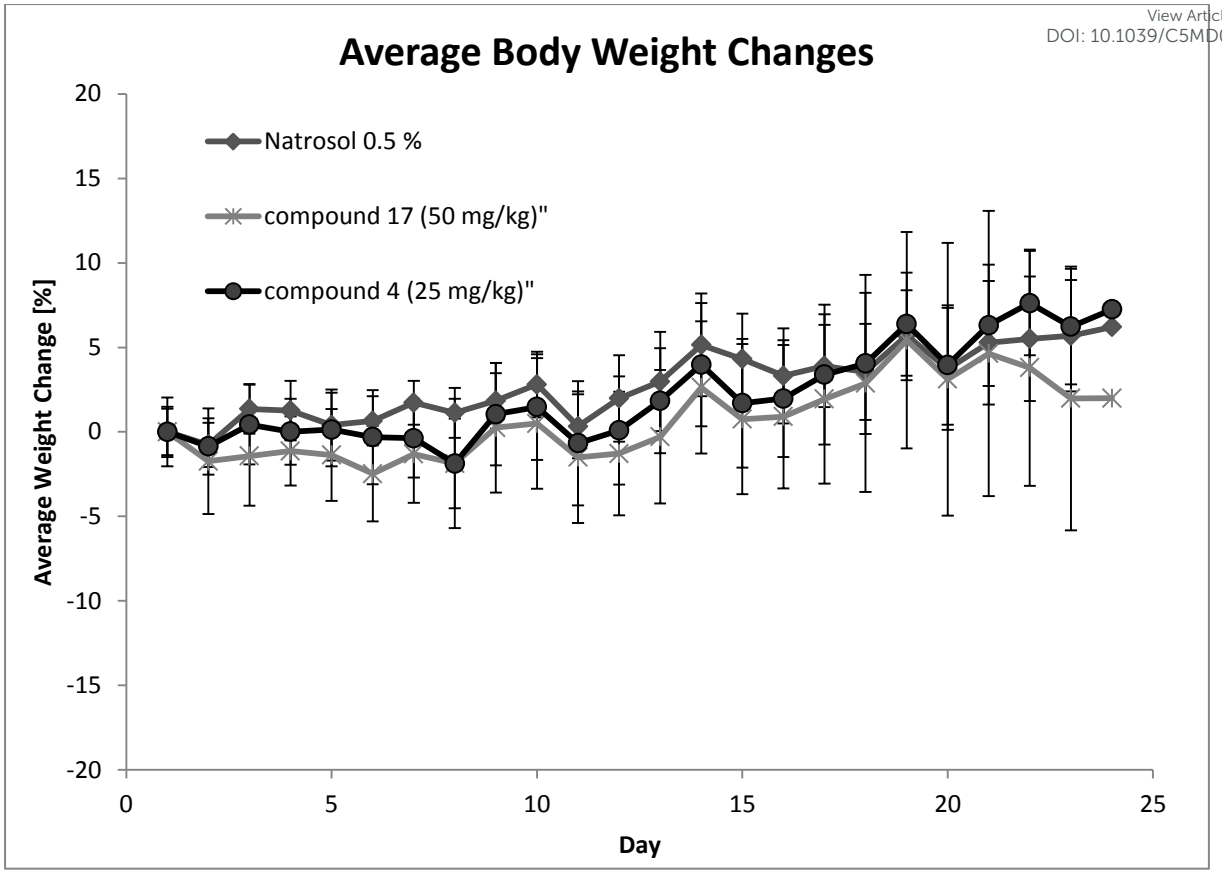

Plot 2 Footnote:

GEO tumor bearing mice were daily treated (p.o.) for 25 days with either 25 mg/kg of compound 4 or 50 mg of compound 17 (i). Both doses were well tolerated as visible by the body weight curves (ii).

In order to confirm that the *in vivo* anti-tumor efficacy of the IGF1R inhibitors was related to target modulation, the effect of an efficacious dose of compound 17 on IGF1R phosphorylation was investigated. GEO tumor-bearing mice were treated once with vehicle or compound 17 (50 mg/kg, p.o.) and the levels of phospho-IGF1R (pIGF1R) in tumors were quantified. Compound 17 led to a statistically significant (p=0.0005) reduction (76% of control) of the pIGF1R signal in GEO tumors at 6 hours after dosing, confirming effective target modulation at this dose level (see figure 5).

Figure 5 – pIGF1R tumor level data for Compound 17

View Article Online
DOI: 10.1039/C5MD00097A

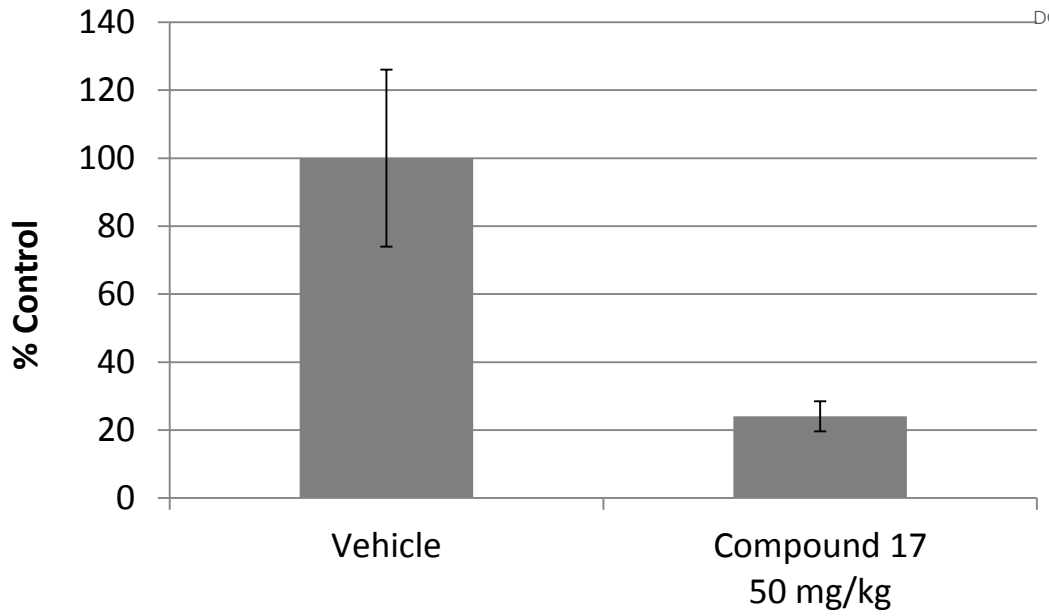

Figure 5 Footnote:

Mice (n=4) bearing GEO tumors were dosed with compound 17 (50 mg/kg po) and sacrificed after 6 hours. Tumors were excised and pIGF1R levels determined and compared to vehicle control.

Conclusion

During our optimization campaign we were able to identify modifications which allowed for the simultaneous improvement of cellular potency and reduction in hERG inhibition. This was enabled by the application of a systematic matched molecular pairs approach coupled with fine tuning of physicochemical properties (principally logD) and the use of a hERG homology model to identify the optimal decoration of the pyrimidine scaffold. The outcome was the identification of compound 17 which met our objectives of having an improved CV safety profile (unbound Cmax to hERG ratio > 100 fold) combined with a cell potency in the nanomolar range. Compound 17 had a good selectivity profile with respect to a panel of kinases and was shown to modulate pIGF levels in tumour tissue which was consistent with the high levels of efficacy achieved in several IGF1R responsive xenograft models.

Acknowledgements

Patricia Amouzegh, Jens Bruchhaus, Sarah Ellam, Thomas Fett, Edward Glenn, Thomas Karner, Stefan Kornigg, Shi Li, Sophie Mitzner, Gurubaran Raju Guido Scholz, Patrick Werni, who made valuable contributions to the synthesis of the compounds.

Thomas Gerstberger, Reiner Meyer, Andreas Schrenk for measuring enzyme and cell activity data.

Stefan Fischer, Astrid Jeschko for performing the *in vivo* studies.

Christian Salamon for performing PK bioanalytics.

Notes and references

1. R. Baserga, *Expert Opin. Ther. Targets*, 2005, **9**, 753-768
2. R. Baserga, F. Peruzzi, K. Reiss, *Int. J. Cancer*, 2003, **107**, 873-877
3. P.J. Beltran, P. Mitchell, Y. A. Chung, E. Cajulis, J. Lu, B. Belmontes, J. Ho, M. M. Tsai, M. Zhu, S. Vonderfecht, R. Baserga, R. Kendall, R. Radinsky, F. J. Calzone, *Mol. Cancer Ther*., 2009, **8**, 1095-1105
4. K. Friedbichler, M. H. Hofmann, M. Kroez, E. Ostermann, H. R. Lamche, C. Koessl, E. Borges, M. N. Pollak, G. Adolf , P. G. Adam, *Mol. Cancer Ther*., 2014, **13**, 399-409
5. (a) J. M. Carboni, M. Wittman, Z. Yang, F. Lee, A. Greer, W. Hurlburt, S. Hillerman, C. Cao, G. H. Cantor, J. Dell-John, C. Chen, L. Discenza, K. Menard, A. Li, G. Trainor , D. Vyas, R. Kramer, R. M. Attar, M. M. Gottardis, *Mol. Cancer Ther*. 2009, **8**, 3341-3349; (b) M. Jin, J. Wang, E. Buck, M. J. Mulvihill, *Future Med. Chem*., 2012, **4**, 315-328; (c) A. Negi, P. Ramana, R. Kumar, *Mini Rev. Med. Chem*., 2013, **13**, 653-681.
6. (a) D. Yee, *J. Natl. Cancer Inst*., 2012, **104**, 975-981; (b) R. Osborne , *Nat. Biotechnol*., 2008, **26**, 719-720
7. E. Buck, P. C. Gokhale, S. Koujak, E. Brown, A. Eyzaguirre, N. Tao, M. Rosenfeld-Franklin, L. Lerner, M. I. Chiu, R. Wild, D. Epstein, J. A. Pachter, M. R. Miglarese, *Mol. Cancer Ther.*, 2010, **9**, 2652-2664
8. (a) E. Buck, M. Mulvihill, *Expert Opin. Investig. Drugs*, 2011, **20**, 605-621; (b) Q. Ji, M. J. Mulvihill, M. Rosenfeld-Franklin, A. Cooke, L. Feng, G. Mak, M. O'Connor, Y. Yao, C. Pirritt, E. Buck, A. Eyzaguirre, L. D. Arnold, N. W. Gibson, J. A. Pachter, *Mol Cancer Ther.,* 2007, **6**, 2158-2167
9. WO2005023780
10. (a) A. M. Aronov, *Drug Discovery Today*, 2005, **10**, 149-155; (b) A. M. Aronov, *Current Topics in Medicinal Chemistry*, 2008, **8**, 1113-1127
11. F. Osterberg, J. Aqvist, *FEBS Lett*., 2005, **579**, 2939-2944
12. A. G. Dossetter, E. J. Griffen, A. G. Leach, *Drug Discovery Today*, 2013, **18**, 724-731

Supporting Information

Details of synthetic procedures, *in vitro* assays and *in vivo* experiments.